

# Selective Tripping at Point of Common Coupling (PCC) Using Inverse-Time Voltage Characteristics

Jai Subbarayan, Brett Cockerham, and Jeremy Blair  
*Schweitzer Engineering Laboratories, Inc.*

Presented at the  
49th Annual Western Protective Relay Conference  
Spokane, Washington  
October 11–13, 2022

Previously presented at the  
75th Annual Georgia Tech Protective Relaying Conference, May 2022  
75th Annual Conference for Protective Relay Engineers, March 2022

Revised edition released March 2022

Originally presented at the  
57th Annual Minnesota Power Systems Conference, November 2021

# Selective Tripping at Point of Common Coupling (PCC) Using Inverse-Time Voltage Characteristics

Jai Subbarayan, Brett Cockerham, and Jeremy Blair, *Schweitzer Engineering Laboratories, Inc.*

**Abstract**—Definite-time voltage-based elements have been commonly applied in applications where a distributed energy resource (DER) interconnects to the electric utility. The purpose of said voltage elements is to isolate the DER from the utility at the point of common coupling (PCC) when abnormal voltage conditions are present. In this paper, we review the use of different operating quantities (phase, positive-sequence, negative-sequence, and zero-sequence voltages) to achieve the best balance between sensitivity and response time for various fault types. Also, this paper introduces the use of inverse-time undervoltage and overvoltage characteristics at the PCC.

In the past, definite-time voltage protection settings have been selected based on point-check calculations, user experience, or with extensive time delays, which can limit the speed, sensitivity, and selectivity. Additionally, the selectivity of operation for these voltage-based elements during faults on the distribution system are difficult to evaluate. This paper proposes a novel and comprehensive method to coordinate definite-time and inverse-time voltage-based protection at the PCC with overcurrent devices deployed in the distribution system. This approach allows a protection engineer to identify the most effective voltage-based protection elements for a given application and discern the relay settings to improve speed, selectivity, and sensitivity at the PCC relay.

The methodology enables faults beyond other protective devices on the distribution feeder to be cleared before the PCC protection operates, allowing the DER to remain grid-connected throughout the disturbance. Finally, we offer the results of rigorous modeling and testing to prove the security, dependability, and selectivity of this new technique.

## I. INTRODUCTION

Inverse-time overcurrent (51) elements, such as phase time overcurrent (51P), ground time overcurrent (51G), and negative-sequence time overcurrent (51Q) elements, have been used extensively in radial distribution systems to establish selectivity in feeder protection while providing secure and dependable protection for feeder faults. As such, the application of these elements to a radial system, in which only one protective device needs to operate to clear a fault and isolate it from all electrical sources, is well-understood in the industry.

However, the introduction of distributed energy resources (DERs) adds a layer of complexity to classical distribution feeder protection. A system that includes a DER is no longer considered to be radial, because the faulted section must be isolated from more than one source. An example DER topology is shown in Fig. 1.

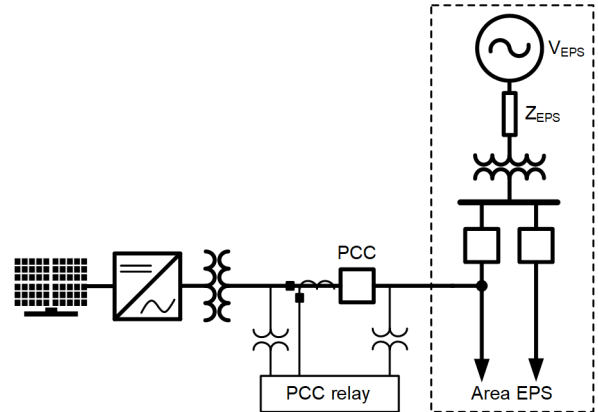


Fig. 1. DER interconnection topology example.

Classically, the means of isolating a faulted section from a DER is done at the point of common coupling (PCC), which includes a recloser or breaker. Directional overcurrent (67) elements can be used in DER applications when sufficient fault current is available to discriminate between load and fault conditions. In such cases, 51 elements that are torque-controlled by a 67 element can be used to selectively coordinate the PCC relay with the distribution system protection for distribution system faults. However, there are known complexities to this arrangement. For example, some inverter-based resources (IBRs) source unstable negative-sequence currents during a fault, making it an unreliable quantity for dependable and secure protection [1]. Additionally, many DER technologies, such as IBR and induction machines, may not contribute more than 1.5 times their rated output [1], and even synchronous machines may contribute less than full rated output after transient fault current contribution has subsided. The PCC relay might also see only a portion of the fault contribution, which can further limit the 51 element's sensitivity and extend its response time.

The dependability of the protection system and its operating times can be improved by using voltage-controlled time overcurrent (51C) or voltage-restrained time overcurrent (51V) elements [2]. However, for DERs that source fault current close to the rated output, the difficulty in establishing dependable and secure protection to coordinate with neighboring devices through the use of current-based elements is apparent [1].

## II. USE OF VOLTAGE RELAYING AT PCC

IEEE Std 1547-2018 (*IEEE Standard for Interconnection and Interoperability of Distributed Energy Resources with Associated Electric Power Systems Interfaces*) defines a DER as “a source of electric power that is not directly connected to a bulk power system” [3]. DERs are often connected directly to distribution feeders, and in some cases are connected directly to distribution substation medium-voltage buses. In most cases, the DER is sized either to support the load of a local electric power system (EPS) or to convert as much of an available power source to electric power as possible. This categorization allows us to note differences in protection requirements between a DER site and any other generation site. Perhaps the most significant difference between the EPS and DERs comes from the high Thévenin source impedance associated with DERs.

DERs can be implemented using a variety of technologies, but every implementation presents a high Thévenin source impedance compared to the area EPS impedances. Even a synchronous rotating machine presents a high Thévenin source impedance compared to the apparent impedance of the many parallel sources that feed the area EPS from the bulk power system. Because of this, the DER contribution of fault current to area EPS faults is often much lower than the contribution from the area EPS itself, and it may be roughly the same for almost any fault on the area EPS. For these reasons, it can be difficult to establish a healthy balance of security and dependability for overcurrent elements at the PCC relay that detects area EPS faults.

Fig. 2a illustrates a typical distribution feeder with a DER connected and shows how we can simplify this circuit to better understand the voltages measured by the PCC during an area EPS fault. In this circuit model, both the area EPS and the DER are represented as Thévenin sources in which the voltage source is an ideal voltage source. If both voltage sources have the same magnitude and angle, then we can simplify the diagram to show a single ideal source (Fig. 2b). With the DER Thévenin source ( $Z_{DER}$ ) impedance now in parallel with the area EPS Thévenin source ( $Z_{EPS}$ ), the fact that  $Z_{DER}$  is so much larger means that it can be approximated as an open circuit (Fig. 2c). At this point, we can observe that the voltage measured at the PCC ( $V_{PCC}$ ) during a bolted fault is effectively the result of a voltage divider between  $Z_{EPS}$  and  $\eta \cdot Z_L$ , where  $Z_L$  is the impedance of the faulted line, and  $\eta$  represents fault location.

Although this approach is just an approximation, it shows that the relay at the PCC experiences large deviations in voltage as the result of downstream feeder faults. Because of this, voltage measurements at the PCC provide a more reliable indication of distribution feeder faults than current measurements. Furthermore, Fig. 2 shows that for unique fault locations, the value of  $\eta \cdot Z_L$  is also unique and creates unique values of voltage measurements at the PCC ( $V_{PCC}$ ). Therefore, the magnitude of  $V_{PCC}$  can be used in establishing criteria to achieve selectivity for area EPS faults.

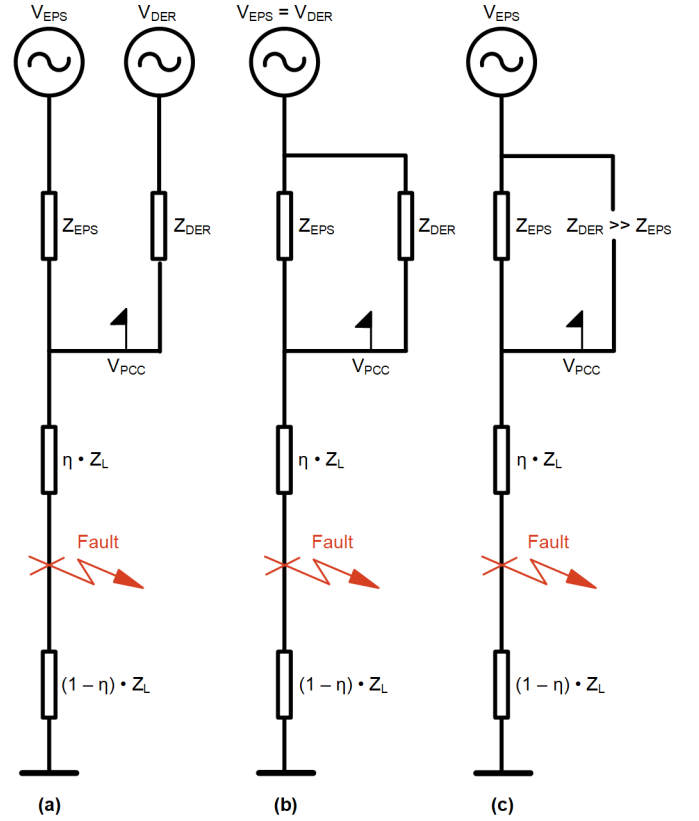


Fig. 2. Simplified circuit for area EPS with DER attached.

However, due to variations in area EPS source strength, fault resistance, and different fault types, voltage magnitudes alone cannot establish selectivity. Time delays must also be used to ensure that the area EPS protection has had a chance to clear the fault before the PCC breaker trips to isolate the DER. Classically, this is achieved through the use of definite-time undervoltage (27) elements applied to line-to-neutral or line-to-line voltages, with time delays to give adjacent feeder protection or recloser controls time enough to clear a fault. If the undervoltage condition still exists after the set amount of time, it is safe to assume that it is located in the section to which the DER is connected, and the PCC breaker must be tripped to isolate the DER from the faulted area EPS. IEEE Std 1547-2018 offers guidance for pickup levels and timer settings of 27 elements, such as those shown in Table I.

TABLE I  
DER SHALL TRIP REQUIREMENTS, CATEGORY I [3]

Shall trip function	Default settings		Ranges of allowable settings	
	Voltage (pu of nominal)	Clearing time (s)	Voltage (pu of nominal)	Clearing time (s)
OV2	1.20	0.16	Fixed at 1.20	Fixed at 0.16
OV1	1.10	2.0	1.10–1.20	1.0–13.0
UV1	0.70	2.0	0.0–0.88	2.0–21.0
UV2	0.45	0.16	0.0–0.50	0.16–2.0

IEEE 1547-2018 offers much more guidance on ride-through capabilities than its predecessors, allowing for a wider range of pickup set points and longer time delays to coordinate with area EPS protection. However, within this wide range of available set points, there is still ample room to reduce isolation speed in response to area EPS faults without sacrificing selectivity. But this standard does not provide any guidance on how such selective operation can be achieved or verified. In many applications, voltage relaying at the PCC has been applied simply based on the default set points in the standard, by point-check calculations to determine the time delays, or by having extensive time delays, all of which compromise the speed, selectivity or sensitivity of voltage relaying at the PCC for faults on the area EPS.

For most utility applications, it is important to reclose soon after an interruption to restore normal service as quickly as possible. But having longer time delays for voltage detection of faults means that the distribution feeder remains energized by the DER for a longer period, which can delay or prevent the feeder protection from reclosing. Therefore, it can be advantageous to trip the PCC breaker as quickly as possible to hopefully restore normal service. Also, it is desirable for the PCC relay to restrain for area EPS faults outside of its zone of protection so that the DER can maintain continuous service. These objectives call for a method that allows users to predict the time of operation of voltage-based protection at the PCC and establish coordination with traditional overcurrent relays for each fault type and for all faults within the area EPS.

### III. COORDINATION OF PCC VOLTAGE PROTECTION WITH AREA EPS 50/51 RELAYS

On radial systems, current-based protection elements are inherently selective, because they operate only for faults downstream of the device. Voltage-based protection elements, however, can operate for faults occurring anywhere on the power system, as long as the operating quantities meet or exceed the pickup requirements. This necessitates a comprehensive study of the protection system to ensure that selectivity is maintained, regardless of the location of the fault. An example distribution system is shown in Fig. 3. Various parameters of this system are provided in Table II, Table III, and Table IV.

Fig. 3 illustrates several fault locations that each respective voltage-based protection element at the PCC relay can potentially operate. This includes faults on the interconnection feeder between the PCC and the distribution substation, such as F5 and F7, and faults downstream of the PCC on the same feeder, such as F8 and F9. Faults on lateral portions of the feeder are identified as F6 and F10, while faults on adjacent feeders are identified as F3 and F4. Substation faults, such as F1 and F2, are also considered.

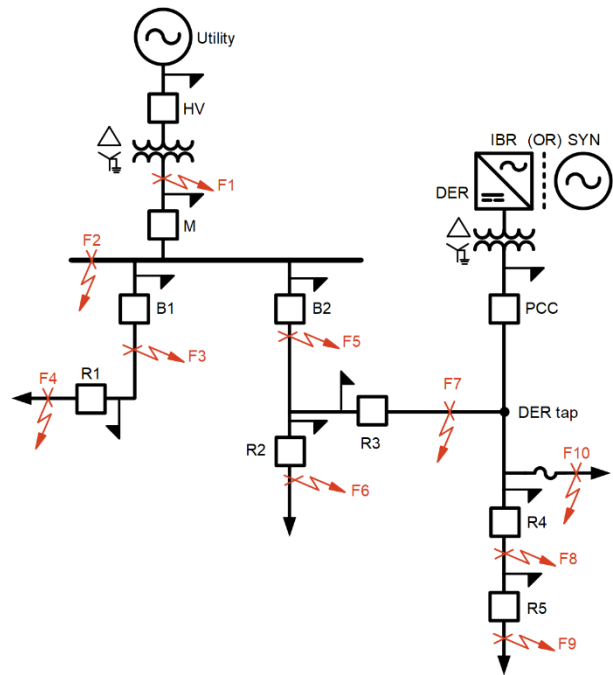


Fig. 3. Model of an example distribution system with DER.

TABLE II  
DISTRIBUTION LINE LENGTHS

From	To	Length (miles)
B2	R2	2
R2	R3	1
R3	TAP	2
TAP	PCC	1
TAP	R4	1
B1	R1	2

TABLE III  
EXAMPLE DISTRIBUTION NETWORK IMPEDANCES\*

Values	Utility	Transformer (pu)	Line (pu/mile)
Rating	34.5 kV	34.5 kV/12.47 kV, 12.5 MVA, Dy1, solidly grounded	2/0 ACSR
Positive-sequence impedance	Infinite source	0.0321 + 0.4975i	0.1619 + 0.6835i
Negative-sequence impedance	Infinite source	0.0321 + 0.4975i	0.1619 + 0.6835i
Zero-sequence impedance	Infinite source	0.0303 + 0.4833i	0.4858 + 2.0504i

\*Impedances are shown in per unit with a base of 100 MVA.

TABLE IV  
SETTINGS FOR CURRENT-BASED RELAYS

Element	Relay	Curve	51 pickup (A)	Time dial	50 pickup (A)
51P	B1, B2	U3	500	0.6	2900
	R2, R3	U3	300	0.9	1120
	R4	U3	250	0.5	900
51G	B1, B2	U3	250	1.2	1900
	R2, R3	U3	200	0.8	830
	R4	U3	175	0.5	550
51Q	B1, B2	U3	400	1.7	4350
	R2, R3	U3	300	1.2	1670
	R4	U3	225	0.5	1330

Based on the fault location, the protection system must respond appropriately to maximize selectivity. The fault locations shown in Fig. 3 are used to understand various permutations of expected relay operation. Table V lists the primary protection device that is expected to isolate the utility source from the respective fault. This table also shows the expected response of the PCC relay to these faults. As shown in Table V, we expect the PCC relay to trip for the faults F1, F2, F5, and F7 to clear the fault. While these faults can be cleared by tripping nearby breakers to remove the utility and DER source, this results in the formation of an unintentional island with the DER as the only source if the PCC breaker is not tripped. So, using the PCC breaker to clear the fault prevents excessive breaker operations. For all other faults, we expect the PCC relay to operate slowly enough to allow the other devices to trip first and maximize selectivity.

TABLE V  
EXPECTED RESPONSE OF THE PROTECTIVE DEVICES

Fault location	Primary device used to isolate substation source	Expected response of PCC relay
F1	HV	Trip
F2	M	Trip
F3	B1	Coordinate with B1
F4	R1	Coordinate with B1
F5	B2	Trip
F6	R2	Coordinate with R2
F7	R3	Trip
F8	R4	Coordinate with R4
F9	R5	Coordinate with R4
F10	Fuse	Coordinate with fuse

Based on Table V, the PCC relay must coordinate with the current-based relays at B1, R2, and R4, as well as with the lateral fuse, for any faults occurring in the zone of protection of these devices. For the fault F6, the PCC relay needs to coordinate with the R2 relay, and not the R3 relay, since R3

measures only the limited current contribution from the DER and may be very slow to operate. If R3 is set based on utility fault levels, this relay may not even pickup for the fault F6.

Ideally, the voltage-based protection at the PCC exhibits the desired selective behavior as determined in Table V. However, there is no existing comprehensive method to evaluate or verify the selectivity of the voltage-based elements at the PCC for faults on the area EPS, other than performing manual calculations.

#### A. Time vs. Normalized Impedance Length Characteristics

This paper proposes the use of time vs. normalized impedance length (TNIL) characteristics to coordinate voltage-based relays to current-based relays for all fault types and various fault locations. We consider the canonical model shown in Fig. 4, which is a simplified distribution system with a DER interconnection, where the utility and DER sources are represented as Thévenin equivalent voltage source and impedance. The definite-time undervoltage relay (27) at the PCC is represented by Relay A, and a current-based 50/51 relay on the area EPS is represented by Relay B.

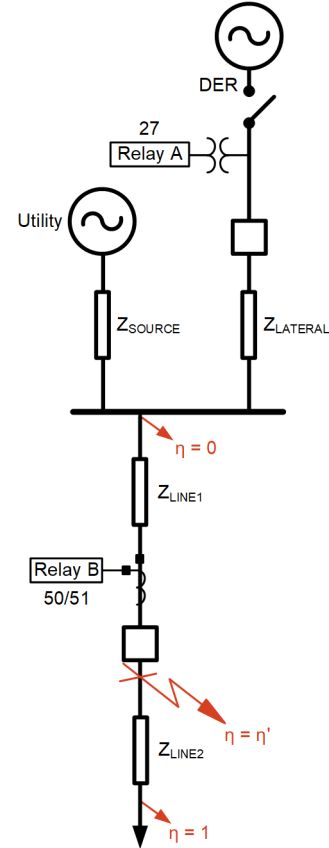


Fig. 4. Canonical model of the coordination pair; Relay A is the voltage-based relay at PCC and Relay B is a current-based device.

For the fault on the protected line as shown in this figure, Relay B is expected to operate first, and Relay A is expected to coordinate with Relay B. The protected line is defined as the distribution line starting from the DER tap point ( $\eta = 0$ ), until the end of the line ( $\eta = 1$ ), where the end is identified by the maximum length for which Relay B is the primary protection

device. If the DER is tapped on a different feeder, then the protected line starts from Relay B ( $\eta = 0$ ).

If the various impedances in this model are known, this model can be solved to calculate the voltage measured at Relay A and the current measured by Relay B. If we consider faults that can occur at any location represented by  $\eta$  along the length of the line on which Relay B is located, we can calculate the fault current seen by Relay B for each of these fault locations, then we can plot the composite response time of the 50/51 relay for each fault location  $\eta$ . Likewise, if we can calculate the voltage seen by a 27 relay at each fault location  $\eta$  for a specific type of fault, we can plot the performance of the 27 relay for each fault location  $\eta$ . In so doing, we can now view the 27 and 50/51 characteristics on the same plane. We call this the TNIL plane, because the X-axis normalizes both voltage and current relay characteristics to an impedance expressed in per unit of protected line length.

Because impedance is used to relate the current and voltage measured by the relaying system for each fault location, we must consider the effects that different fault types have on the measured apparent impedance. The measured impedance of a phase-to-phase fault loop is much different than the impedance of a phase-to-ground fault loop or a three-phase fault loop for the same fault location [4]. So, for the purposes of coordinating voltage and current relays on a three-phase power system, we must map the 27 and 50/51 characteristics to a unique TNIL plane for each of the four fault types (three-phase [3P], phase-to-phase [LL], single-phase-to-ground [1LG], and LLG). In doing so, we find that the 27 and 50/51 characteristics for each operating quantity can take on a different response in the TNIL plane for each fault type.

Fig. 5 is used to illustrate the characteristic response of the 27 element on the PCC relay (Relay A) and 50/51 elements on the R4 relay (Relay B) in the example distribution system using the three-phase (3P) TNIL plane. The characteristic plots on this figure represent the time of operation of Relays A and B for metallic three-phase faults on the protected line. The X-axis is extended beyond the protected line ( $\eta > 1$ ) to represent resistive faults. In Fig. 5, the default IEEE 1547 “shall trip” requirement set points are used for the 27 elements on the PCC. The settings for R4 are given in Table IV.

For faults  $\eta < \eta'$ , 50/51 relay does not operate as these faults are behind the 50/51 relay. For these faults, the UV2 27 relay at PCC trips fast. But for faults below Relay B ( $\eta \geq \eta'$ , as shown in Fig. 4), the UV2 27 relay does not coordinate with R4. This miscoordination unnecessarily removes the DER from service.

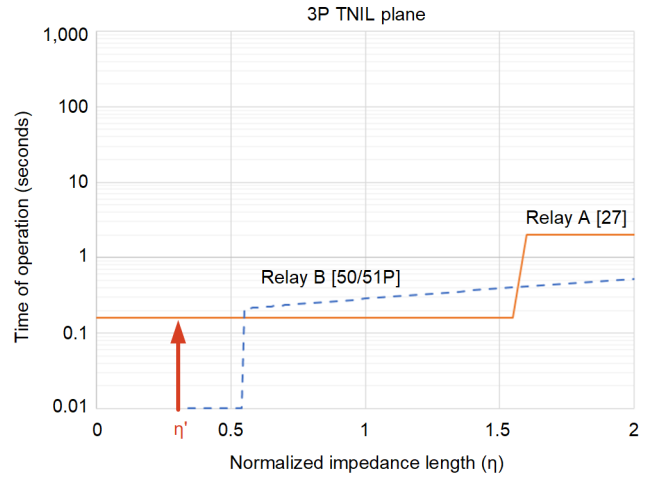


Fig. 5. Characteristic response of PCC (Relay A) and R4 (Relay B) relays for three-phase faults on the protected line plotted on the 3P-TNIL plane.

The TNIL plane acts as a visualization tool in determining if the voltage protection at the PCC properly coordinates with the overcurrent devices in the area EPS. Additionally, it introduces a way to coordinate the 27 elements at the PCC relay with a downstream current-based relay such as R4. The PCC relay should maintain coordination with R4 for all fault types occurring at  $\eta \geq \eta'$ . In addition to 51P, the R4 relay also incorporates 51G and 51Q elements. The 27 elements at the PCC relay should coordinate with these overcurrent elements as well. Furthermore, the 27 protection at the PCC relay should coordinate with multiple current-based devices on the area EPS, as described in Table V. One option is to eliminate the use of the UV2 27 element and use only the UV1 element with a long time delay, but this approach sacrifices the speed of operation. A second option is to replace the UV2 with an alternative voltage-based characteristic that better serves in coordination without compromising operating times.

### B. Inverse-Time Characteristics

The need to balance speed, sensitivity, and selectivity is not new. This need has been met in many protective relay system designs. One commonly applied relay element is the inverse-time overcurrent (51) element, in which the operating time of the characteristic is inversely related to the magnitude of the fault current. Because of this relationship, higher current magnitudes result in faster operating times (Fig. 6).

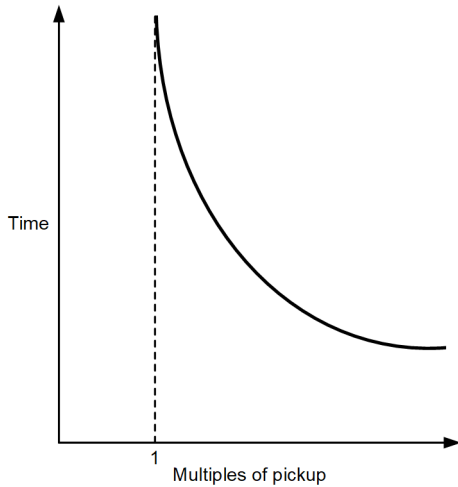


Fig. 6. Time vs. current example characteristic plot for a 51 relay.

With digital relays, the same principle can be applied to any measurable or calculated quantity. As detailed in Fig. 2, voltage measurements at the PCC can yield greater sensitivity to area EPS faults than current measurements, and the inverse-time relationship applied to any operating quantity offers a natural balance of speed, sensitivity, and selectivity. Definite-time relays can further improve speed of operation by limiting the time of operation for resistive faults which result in less severe changes in voltage. The combination of inverse-time and definite-time voltage relaying at the PCC offers the best local measurement-based solution to trip the PCC breaker as quickly as possible for feeder faults that require isolation of the DER, while also ensuring that the PCC remains closed for utility faults cleared by remote protection using inverse-time (51) and definite-time (50) overcurrent elements.

The inverse-time undervoltage (27I) characteristic is well-established and available to protection engineers in discrete forms and in modern multifunction digital relays. As with inverse-time overcurrent relays, we set a pickup, and the operating time of the relay is inversely proportional to the deviation of the measured current from the set pickup. However, for a 27I relay the operating quantity is voltage and the deviation is taken as inverse multiples of pickup. Therefore, as the measured voltage magnitude decreases below the set pickup, the operating time also decreases. Fig. 7 illustrates this voltage-based characteristic.

Faults closer to the relay produce a more severe voltage drop, resulting in faster operating times while faults further downstream from the relay produce a less severe voltage drop, which leads to slower operating times. This behavior provides a natural means of selectivity based on time of operation.

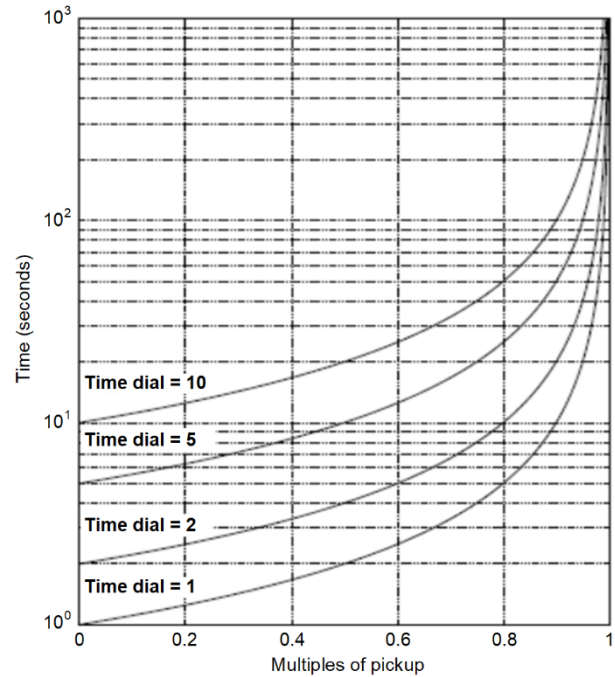


Fig. 7. Time vs. voltage example characteristic plot for a 27I relay [5].

Based on this premise, a 27I relay was used on PCC, along with the UV1 27 relay to achieve coordination with the R4 relay, as shown in Fig. 8.

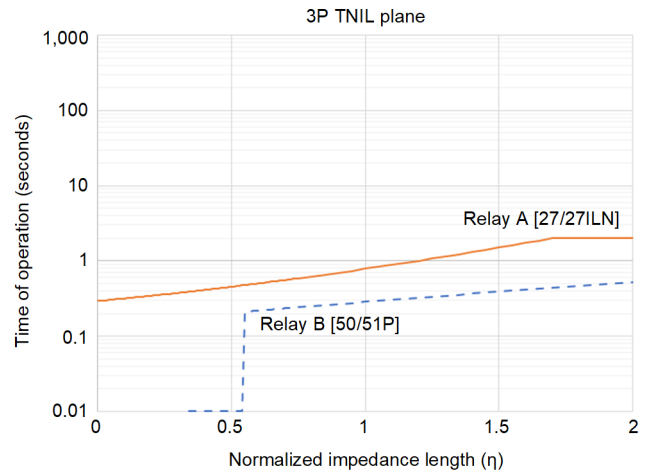


Fig. 8. Using 27ILN for coordination between PCC and R4 relays on the 3P-TNIL plane.

The 27ILN element at the PCC allows the PCC trips fast for close-in three-phase faults ( $<0.3$  seconds) while maintaining coordination for faults below R4, while the UV1 27 element provides reliable operation for resistive faults with a longer time delay (2 seconds).

### C. Voltage Relay Operating Quantities

Up to this point in the paper, we have referred to the operating quantity of 27 and 27I relays as simply voltage. However, we can use minimum line-neutral voltage ( $V_{MIN}$ ) for 27ILN relays or minimum line-to-line voltage ( $V_{MINLL}$ ) for 27ILL relays. A 27ILN relay provides greater sensitivity to ground faults, while a 27ILL relay provides greater sensitivity to phase faults. For three-phase faults, an identical response is expected for 27ILN and 27ILL relays with identical per-unit settings. This introduces the concept that other operating quantities may be best suited to specific fault types. This is a traditional concept understood and applied in overcurrent protection, in which a zero-sequence or ground overcurrent (51G) element is applied for detection of ground faults, a negative-sequence overcurrent (51Q) element is applied for detection of phase (excluding three-phase) and ground faults, and a phase overcurrent (51P) element is applied for phase faults (including three-phase faults) [6].

Another advantage to using 51G and 51Q relays in overcurrent relaying is that the operating quantity ( $3I_0$  and  $3I_2$  for the respective relay types) is usually zero or near zero during normal power system operation, allowing for very sensitive pickup settings. Likewise,  $3V_0$  and  $3V_2$  are near zero under normal balanced conditions. As such, users can use these elements to set a voltage relay responding to  $3V_0$  or  $3V_2$  voltage much more sensitively to provide the most sensitive coverage for ground and unbalanced fault types.

It is expected that  $3V_0$  and  $3V_2$  increase during a fault, so to detect faults using these quantities, overvoltage relays (59G and 59Q, respectively) must be used. To apply the inverse-time characteristic to ground and unbalanced faults, an inverse-time overvoltage (59I) relay can be employed that uses  $3V_0$  (59IG) and  $3V_2$  (59IQ) as operating quantities. Fig. 9 shows a typical 59I characteristic on the time versus voltage plane.

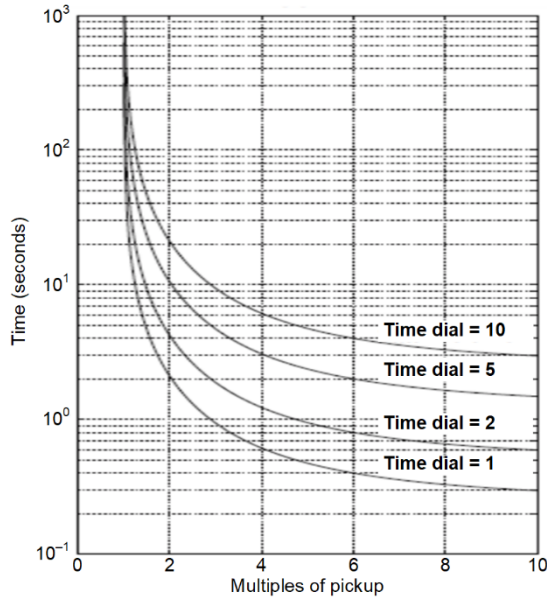


Fig. 9. Time vs. voltage example characteristic plot for a 59I relay [5].

If a 51Q relay is not available, the 51P relay provides the only overcurrent means of detecting faults not including ground, and the 59IQ relay must then be coordinated with the 51P relay. Like the 27I characteristic, the 59I response can be mapped to the TNIL plane for coordination purposes. While developing these coordination diagrams, we determined that the 27/27ILN, 59G/59IG, and 59Q/59IQ elements provide the simplest coordination with 50/51P, 50/51G, and 50/51Q elements, respectively. Fig. 10 shows the implementation of 59Q/59IQ on the PCC relay and the coordination with 50/51Q elements on the R4 relay using the LL-TNIL plane.

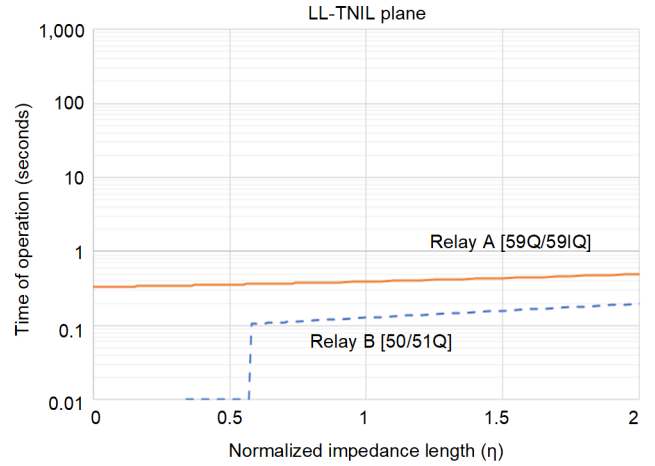


Fig. 10. Coordination of negative-sequence elements on PCC and R4 relays using the TNIL plane.

### D. Coordinating Multiple Voltage and Current Relays for All Fault Types

For some unbalanced faults where both zero-sequence and negative-sequence quantities are generated in substantial amounts, such as an LLG fault, the voltage-based relays (27/27I, 59G/59IG, and 59Q/59IQ) are effectively racing against each other, similar to how 50/51P, 50/51G, and 50/51Q elements race against each other. To ensure that coordination is achieved for types of faults, regardless of which protective element wins the race, the composite behavior of the elements in Relay A is compared against the composite behavior of the elements in Relay B. Fig. 11 shows an example of coordinating Relays A and B on the LLG-TNIL plane in which all protective elements in both relays respond, but the ground elements win the race.

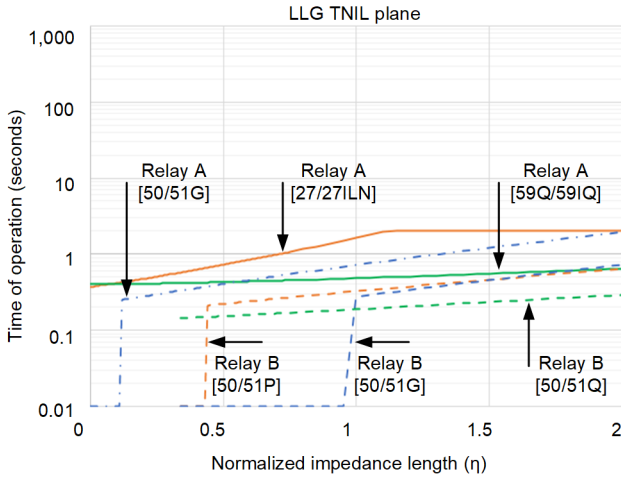


Fig. 11. LLG-TNIL characteristic example for all available 27/27I, 59/59I, and 50/51 relays.

The composite characteristic behavior of Relays A and B can be drawn to simplify Fig. 11, as shown in Fig. 12.

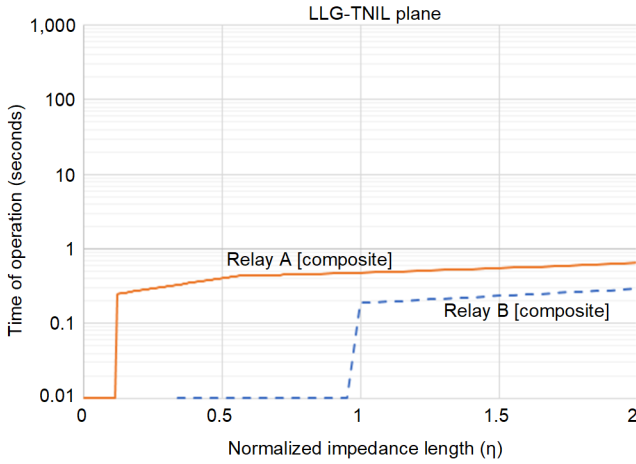


Fig. 12. Composite characteristics of Relays A and B on the LLG-TNIL plane.

### E. Canonical Model of the Coordination Pairs

To plot the TNIL characteristics of any current-based or voltage-based relay, knowledge of the source and line impedances is required to estimate the operating quantities that are measured by these relays for faults occurring on the protected line. In this paper, the canonical model shown in Fig. 4 is used to reduce the distribution system into equivalent impedances to perform the necessary calculations for plotting the TNIL characteristics.

In this model, Relay A is fixed as the voltage-based PCC relay, and Relay B represents any current-based relay with which the PCC relay is required to achieve coordination. The various impedances shown in this model are chosen based on the path of the fault current contribution from the strong utility source for faults downstream of Relay B, as shown in Fig. 4. The source ( $Z_{SOURCE}$ ) represents the path of this fault current that is upstream to both Relays A and B. Line 1 ( $Z_{LINE1}$ ) represents the path of this fault current between Relay A and Relay B, while Line 2 ( $Z_{LINE2}$ ) represents the path of this fault current downstream of Relay B. The lateral path between

Relay A and the path of the fault current from the utility is represented as the lateral impedance ( $Z_{LATERAL}$ ) in this canonical model. For faults occurring downstream of Relay B, Relay A and Relay B must coordinate to maintain selectivity.

As explained in Section II, the Thévenin impedance of the area EPS source ( $Z_{EPS}$ ) is much smaller than the Thévenin impedance of the DER ( $Z_{DER}$ ), so the influence of the DER source is not considered while performing coordination. Hence, the canonical model consists of only one positive-sequence source, and the DER source is assumed to be open-circuited. Results from extensive simulations (see Section V) have shown that DER sources with high source impedance compared to the area EPS have minimal influence on the associated operating quantities, thereby validating this approximation. Results have also shown that inverter-based DERs have even less influence on the quantities seen by Relay A and Relay B. The effect of load flow is also ignored.

Table V establishes the coordination requirements of the PCC relay to various protective devices on the example distribution system in Fig. 3. We consider the case of the coordination requirement between the PCC and R4 relays. For faults occurring downstream of R4, the PCC relay is expected to coordinate with R4. Using the canonical model proposed in Fig. 6, the distribution system is reduced to conform to the canonical model as shown in Fig. 13a. For a fault downstream of Relay B, the fault current from the utility flows through the substation transformer, the bus, Line B2-R3, Line R3-DER Tap, Line DER Tap-R4, and finally, from R4 to the fault location. In this fault network, the impedance upstream of the DER Tap point determines the voltage at the PCC, and this impedance is reduced to  $Z_{SOURCE}$ . The fault current is determined by the impedance of the entire fault path. The impedance between Relays A and B is reduced into  $Z_{LINE1}$  and the impedance to the fault from R4 is reduced to  $Z_{LINE2}$ . The impedance between the fault path and the PCC relay is reduced to  $Z_{LATERAL}$ . Since no current flows in this path,  $Z_{LATERAL}$  does not influence the voltage measured at PCC. In cases where a zero-sequence source is present at the PCC, zero-sequence current flow through  $Z_{LATERAL}$  and for such cases this input is required to calculate the operating quantities for Relays A and B as discussed later in this section.

Fig. 13b illustrates how to reduce the distribution system to conform to the canonical model to perform coordination between the PCC and B1 relays. In this case, the fault current from the utility source flows through the substation and directly on to the faulted line below B1. While the interconnecting feeder (B2-R3-DER Tap) connects the DER to the faulted path, it does not carry any current based on the assumption that the DER is open-circuited, and hence it cannot be included in  $Z_{LINE1}$ . Therefore, this impedance is lumped into the  $Z_{LATERAL}$  impedance. The voltage at PCC is determined by the voltage drop across the utility source and substation transformer impedance, and hence these are combined as  $Z_{SOURCE}$ . Since there is no fault current carrying impedance between  $Z_{SOURCE}$  and B1,  $Z_{LINE1}$  is considered as zero. The impedance below B1 is reduced to  $Z_{LINE2}$ .

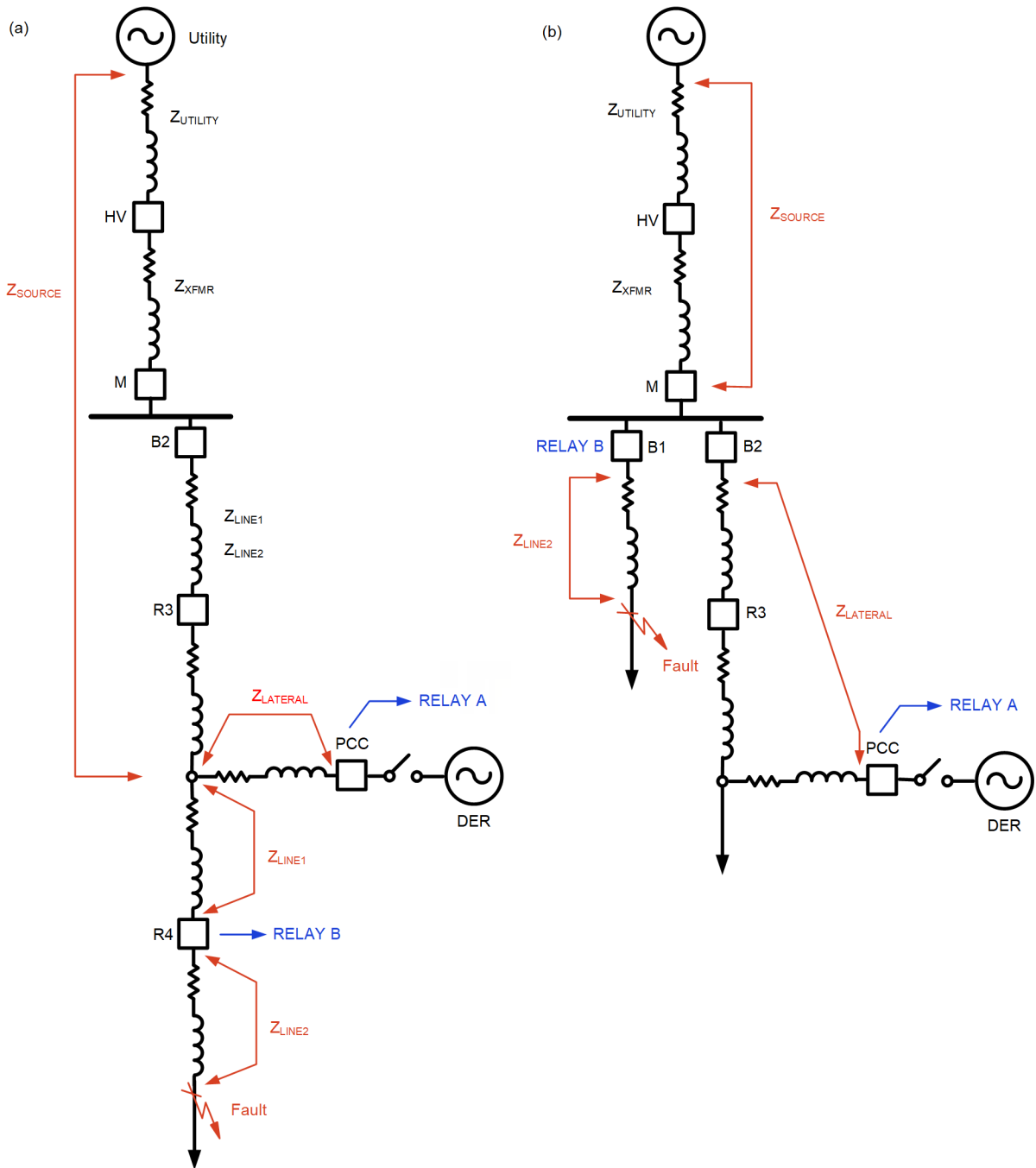


Fig. 13. Canonical model for coordination between relays (a) PCC and R4 (b) PCC and B1.

It can be observed that Table VI lists the source, Line 1, Line 2, and lateral impedances for all the coordination pairs (as dictated by Table V).

TABLE VI  
CANONICAL MODEL IMPEDANCES FOR VARIOUS COORDINATION PAIRS

Coordination Pair	$Z_{SOURCE}$ ( $\Omega$ )	$Z_{LINE1}$ ( $\Omega/mile$ )	$Z_{LINE2}$ ( $\Omega/mile$ )	$Z_{LATERAL}$ ( $\Omega$ )
PCC-R4	Utility source + transformer + Line B2- DER TAP	DER TAP-R4	Line R4-R5	DER TAP-PCC
PCC-B1	Utility source + transformer	0	Line B1-R1	DER TAP-PCC + Line B2- DER TAP
PCC-R2	Utility source + transformer + Line B2-R2	0	Line R2	DER TAP-PCC + Line R2- DER TAP
PCC-fuse	Utility source + transformer + Line B2- DER TAP	DER TAP-fuse	Line downstream of fuse	DER TAP-PCC

The horizontal axis (X-axis) of the TNIL curve (Fig. 5) represents the faulted length of the protected line, normalized by the total length of the line. The total length of the protected line is considered to be the sum of the Line 1 length and Line 2 length (in miles). Continuing with the example of coordination between PCC and R4, the total line length is the length of the distribution line from DER tap to R5. The variable  $\eta$  is used to represent the normalized impedance length in this paper, which is defined by the formula in (1).

$$\eta = \frac{\text{Distance of fault from DER tap}}{\text{Line 1} + \text{Line 2}} \quad (1)$$

In cases where there is no Line 1, such as the coordination between PCC and B1, the numerator in (1) can instead be considered the distance of the fault from Relay B, as shown in (2).

$$\eta = \frac{\text{Distance of fault from Relay B}}{\text{Line 2}} \quad (2)$$

The calculation of operating quantities measured by Relay A and Relay B for various fault types and locations along the protected line is provided in Appendix A through D.

#### F. The Effect of an Additional Zero-Sequence Source at PCC

It is common for a delta-wye-grounded transformer to be used when connecting the DER to the distribution system. This transformer connection can create a new low-impedance path for zero-sequence current to flow. Under such conditions, the effect of this new zero-sequence path must be considered in the calculation of the operating quantities for Relays A and B since this transformer connection is a zero-sequence source. Calculations for faults that do not involve the zero-sequence

network remain unaffected, while 1LG and LLG fault calculations are significantly affected. An illustration for how the canonical model is adjusted to account for a transformer connection that yields a zero-sequence path is shown in Fig. 14. The flow of zero-sequence current from the PCC causes a voltage drop across  $Z_{LATERAL}$ , making this a necessary input for the calculations. The modified calculation of operating quantities measured by Relay A and Relay B for ground faults at various locations along the protected line is provided in Appendix E and F.

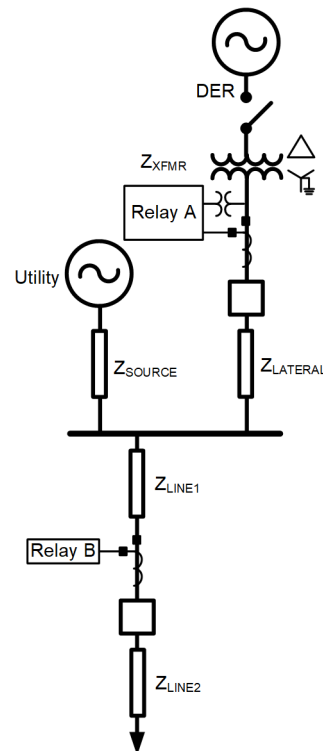


Fig. 14. Canonical model form of the coordination pair that includes an additional ground source at the DER PCC.

The use of an additional ground source at the PCC can reduce the zero-sequence impedance behind Relay A. As a result, the zero-sequence voltage seen by Relay A for a ground fault is low, regardless of the fault current, and is therefore not a very reliable operating quantity. Because the ground connection ultimately sources zero-sequence current from the utility positive-sequence source, the fault currents are comparable to those supplied from the utility source rather than what is supplied by the DER.

Based on this, a 50/51G element is a more appropriate choice for ground fault protection on Relay A, which can be coordinated on the 1LG-TNIL plane with the 50/51G element on Relay B.

While time-current characteristic (TCC) curves are normally used to coordinate two current-based protection elements, the TNIL-plane-based coordination is useful since Relay A and Relay B are expected to measure differing ground current.

The 51G element on Relay B operates on the total fault zero-sequence current, and the 50/51G element on Relay A only observes a fraction of this zero-sequence current. This is

illustrated in Fig. 15. The calculation of the zero-sequence current seen by Relay A is shown in Appendix E.

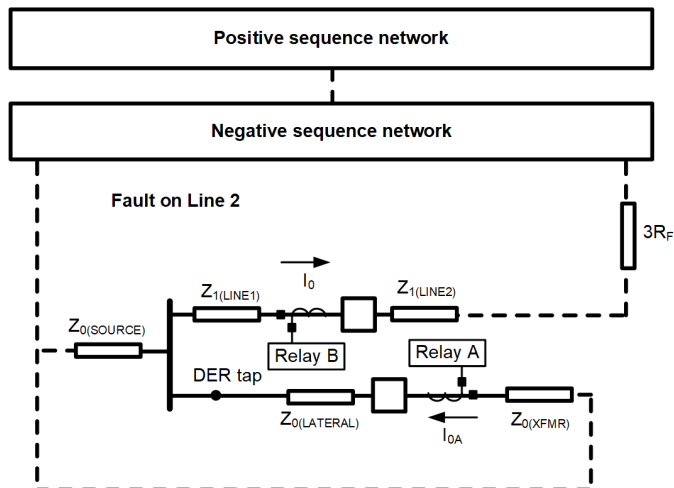


Fig. 15. Splitting of zero-sequence current contribution for a ground fault on Line 2.

For the fault F6 in Fig. 3, Relay R3 now measures significant zero-sequence current contribution from the PCC transformer, which may lead to the trip of Breaker R3. While it may be desirable to coordinate R3 for ground faults in the reverse direction with R2, an operation of R3 requires a PCC trip to prevent islanding the DER with the area EPS downstream of R3. Hence, coordinating the 50/51G on R2 directly with a 50/51G on the PCC relay is desirable. In this case, R3 should incorporate forward ground directional supervision to avoid operating for F6.

#### G. When Relay B Is a Fuse

As identified in Table V and Table VI, fuses on laterals also have to coordinate with the PCC relay for faults on the lateral feeder. When fuses are used to protect a lateral feeder, these fuses are generally very fast, because in most cases they are sized to coordinate with line reclosers. While it might be reasonable to assume that fuses operate faster than the PCC relay, this section establishes a mathematical approach to plotting the fuse curve on a TNIL plane, which helps to ensure that a lateral feeder fuse does coordinate with the PCC relay.

Fuses always use phase current as the operating quantity; therefore, the formulae used for the  $I_f$  calculation in the Appendix can be used (for all types of faults). Although a characteristic equation for the time of operation is usually not available for fuses, the TCC curve of a fuse can be converted to a set of two-dimensional data points consisting of current and time of operation. Using the  $I_f$  formulae (Appendix), the operating current is calculated for the fuse. The time of operation can be calculated approximately by performing an interpolation based on the data points obtained from the TCC curve. To maintain accuracy, linear interpolation can be performed between two data points closest to the operating current ( $\forall 0 \leq \eta \leq 2$ ). Alternatively, inverse-square curve fitting can also be performed to obtain a characteristic expression for the total clearing time of operation of the fuse as a function of current.

#### H. Evaluating PCC Relay Compliance to IEEE Std 1547 Ride-Through Requirements

IEEE Std 1547 establishes the minimum ride-through requirements for disturbances on the area EPS, during which the PCC relay is expected not to trip, as shown in Table VII, for a Category I system. The standard can be referenced to determine the appropriate category. This calls for the evaluation of compliance by the PCC relay to these ride-through requirements. The protection elements used at the PCC should not operate faster than the minimum time of operation as specified in the ride-through requirements. The standard provides the minimum time of operation for various levels of per-unit voltage. The standard allows the “voltage” in Table VII to be either line-to-neutral or line-to-line voltage, based on the type of protection element being used. Since the line-to-neutral elements are used in this paper, this minimum time of operation is plotted on the TNIL plane for various faults on the protected line based on the minimum line-to-neutral voltage. To ensure compliance, the time of operation of 27/27ILN has to be larger than the minimum time of operation as specified in the standard. In Fig. 16, the 27/27ILN element on the PCC relay is coordinated with the 50/51P element on B1 relay, for three-phase faults occurring downstream of B1. The applicable operating quantities are calculated using the equations provided in Appendix A. The minimum time of operation as specified in Table VII is plotted and identified as “1547 ride through.”

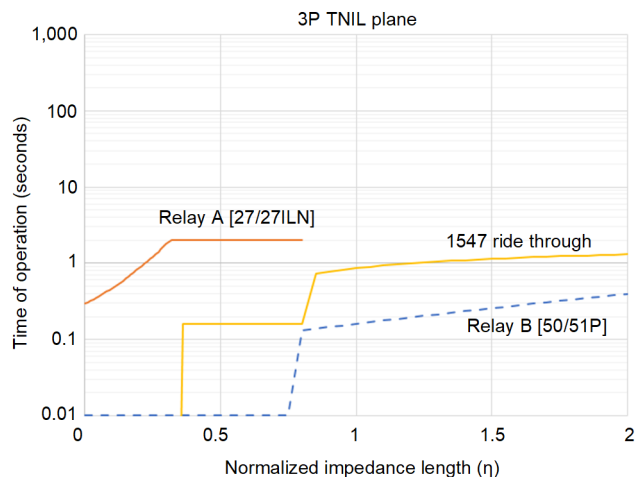


Fig. 16. IEEE 1547 minimum time of operation for PCC to ride through area EPS 3P fault.

The 27/27ILN time of operation exceeds the minimum time of operation as specified in Table VII. Similar evaluations can be performed for unbalanced faults using other TNIL planes to ensure that the 27/27ILN element operates slower than the ride-through requirements for all types of faults.

TABLE VII  
VOLTAGE RIDE-THROUGH REQUIREMENTS FOR DER (CATEGORY I)

Voltage range (pu)	Operating mode/response	Minimum ride-through time (s) (design criteria)
$V > 1.20$	Cease to energize	N/A
$1.175 < V \leq 1.20$	Permissive operation	0.2
$1.15 < V \leq 1.175$	Permissive operation	0.5
$1.10 < V \leq 1.15$	Permissive operation	1
$0.88 \leq V \leq 1.10$	Continuous operation	Infinite
$0.70 \leq V < 0.88$	Mandatory operation	*
$0.50 \leq V < 0.70$	Permissive operation	0.16
$V < 0.50$	Cease to energize	N/A

\* Linear slope of 4 s/1 pu voltage starting at 0.7 s at 0.7 pu:

$$T_{VRT} = 0.7 \text{ s} + \frac{4 \text{ s}}{1 \text{ pu}} (V - 0.7 \text{ pu})$$

The use of 59/59G and 59/59Q protection elements on the PCC relay means that these elements can operate faster than the 27/27ILN elements for unbalanced faults on the area EPS. Similarly, a 50/51G element on the PCC relay can operate faster for ground faults on the area EPS as compared to the 27/27ILN element. Since these protection elements can trip the PCC relay for system disturbances, these elements should also be evaluated for compliance to ride-through requirements. For the low-voltage ride-through requirements, IEEE 1547 allows the “voltage” in Table VII to be interpreted as any applicable quantity among the line-to-neutral, line-to-ground and line-to-line voltage, which has the least magnitude.

During line-to-line faults, the line-to-line voltage experiences the most change in operating quantity, and so the minimum line-to-line voltage ( $V_{LL(MIN)}$ ) is used to determine the minimum ride-through requirement. Fig. 17 shows the coordination of the 59/59IQ element on the PCC relay to the 50/51Q element on B1 for line-to-line faults occurring downstream of B1.

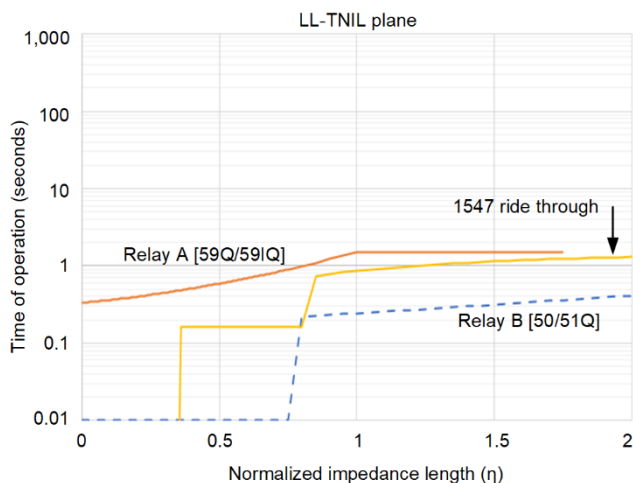


Fig. 17. IEEE 1547 minimum time of operation for PCC to ride through the area EPS LL fault.

For 1LG faults, the minimum line-to-neutral voltage can be used to determine the minimum ride-through requirement,

similar to three-phase faults, since  $V_{LN}$  experiences a larger deviation from the nominal, as compared to  $V_{LL}$ . The same evaluation is performed for all coordination cases specified in Table V. It is important to note that this compliance does not require a “coordination interval” and having the time of operation be equal to or greater than the minimum time of operation is sufficient.

#### IV. VOLTAGE ELEMENT SETTING GUIDELINES

By applying the equations in Appendices, the operating quantities for Relays A and B can be calculated for various combinations of protective elements—using the impedances shown in Table III and the line lengths shown in Table II—for the example distribution system depicted in Fig. 3. The time of operation for these relays can then be calculated based on the associated curve settings for  $0 \leq \eta \leq 2$ .

A complete step-by-step procedure for performing the coordination is described in the following steps:

1. Evaluate the coordination requirement as shown in Table V and choose the case where the current-based relay is electrically closest to the DER tap point. For example, the distribution system in Fig. 3 is a case of coordination between PCC and R4 relays.
2. To determine the inverse-time voltage pickups, find the value of  $\eta$  for each fault type ( $\eta_{3P}$ ,  $\eta_{LL}$ , and  $\eta_{LG}$ ) at which the fault current magnitude is approximately equal to 150 percent of the respective 51 pickup (51P, 51Q or 51P, 51G) of the feeder protective relay or recloser control.
3. Using traditional overcurrent coordination methods, coordinate the voltage-based elements with the current-based elements by specifying the curve and time dial for the inverse-time voltage characteristic on the respective TNIL plane.
4. Coordinate 27ILN with 51P on the 3P-TNIL plane with the pickup of 27ILN equal to the minimum line-neutral voltage at the PCC for a fault at  $\eta_{3P}$ . The variable  $\eta_{3P}$  is calculated with fault current equal to 150 percent of the pickup of 51P, as described in Step 1. Ensure that this pickup is lower than the minimum line-neutral voltage at worst-case emergency loading to prevent a DER trip on load conditions.
5. Determine whether 51Q is active in the area EPS protective relay.
  - If so, coordinate 59IQ with 51Q on the LL-TNIL plane with the pickup of 59IQ equal to the negative-sequence voltage at the PCC for a fault at  $\eta_{LL}$ . To include margin,  $\eta_{LL}$  is calculated with fault current equal to 150 percent of the pickup of 51Q.
  - If not, coordinate 59IQ with 51P on the LL-TNIL plane with the pickup of 59IQ equal to the negative-sequence voltage at the PCC for a fault at  $\eta_{LL}$ . To include margin,  $\eta_{LL}$  is calculated with fault current equal to 150 percent of the pickup of 51P.

- Ensure that the 59IQ pickup is higher than the maximum negative-sequence voltage at worst-case load unbalance.
- 6. Coordinate 59IG with 51G on the 1LG-TNIL plane with the pickup of 59IG so that it is equal to the zero-sequence voltage at the PCC for a fault at  $\eta_{LG}$ . To include margin,  $\eta_{LG}$  is calculated with fault current equal to 150 percent of the pickup of 51G. Ensure that the 59IG pickup is higher than the maximum zero-sequence voltage at worst-case load unbalance.

The pickup thresholds for voltage relays at the PCC are calculated to match the reach of the current relays with some margin. Since the voltage-based Relay A is located upstream of the current-based Relay B, Relay A can have a lower reach into the protected line as compared to Relay B. The scaling factor of 150 percent represents the amount by which the reach of the voltage-based relay is pulled back from the reach of the current-based relay. If a scaling factor of 100 percent is used, then the two relays have the same reach, which makes the voltage-based relay overly sensitive and difficult to coordinate.

- 7. The UV1 definite-time voltage-based relays (27, 59G, 59Q) can be used to provide dependable protection for resistive faults, by choosing a sensitive set point combined with a long time delay. To set the pickup for 27, 59G and 59Q, recalculate  $\eta_{3P}$ ,  $\eta_{LL}$ , and  $\eta_{LG}$  for a fault current equal to 125 percent of the respective 51 pickup. Consider conditions such as worst-case emergency loading, worst-case load unbalance and transient conditions such as transformer inrush (when applicable) to secure these definite-time elements.
- 8. Based on the settings obtained from Steps 1 through 8 for Relay A, plot the composite characteristic response for each type of fault as shown in Fig. 18.
- 9. Set the definite-time delay for UV1 27, 59G, 59Q elements such that the composite characteristic response of the Relay A maintains coordination with Relay B for all types of faults.
- 10. If inverse-time voltage characteristics are not available on the PCC relay, then UV2 definite-time voltage-based relays (27, 59G, 59Q) can be used instead to provide fast operation for nearby metallic faults. Select a pickup and definite-time delay that satisfies the IEEE 1547-2018 UV2 trip requirements. Ensure that this element coordinates with Relay B for all fault types using the TNIL plane.
- 11. Choose the coordination requirement where the current-based relay is electrically closest to the utility

source. The example distribution system in Fig. 3 is a case of coordination between PCC and B1 relays. Repeat Step 9. In most cases, the settings obtained from the first coordination case should continue to maintain coordination. If not, Relay A settings can be desensitized by increasing the time dial or definite-time delay.

- 12. For this coordination case, plot the IEEE 1547 ride-through requirements along with the composite characteristic curves to ensure compliance by the PCC relay. Increase the UV1 27 time delay if needed. In most cases, if the PCC relay maintains compliance for this coordination case, it maintains compliance for other cases.
- 13. Repeat Step 8 for all other cases of coordination. In most typical cases, no more adjustments should be required.

The resulting composite curves for coordination between PCC and R4 relays are shown in Fig. 18a through Fig. 18d. The resulting settings (from coordinating the PCC relay to all devices as required in Table V) are shown in Table VIII. A 2 MVA, 600 V/12.47 kV delta-wye-grounded transformer is used for the DER interconnection, which requires the use of a 51G element at the PCC instead of a 59/59IG element.

TABLE VIII  
RESULTING SETTINGS FOR RELAY A (PCC)

Element	Curve	Pickup (V)	Time dial	Definite-time pickup	Definite-time delay (s)
27/27ILN	CURVEB	4800	0.13	88	2.0
50/51G	U3	125 A	1.2	3	0.0
59/59IQ	CURVEA	2040	0.3	30	1.5

## V. TESTING THE COORDINATION SCHEME

The example distribution system described in Table II, Table III, and Fig. 3 was modeled in MATLAB/Simulink for three different cases, as described in Table IX.

TABLE IX  
TEST CASES

Test cases	DER source
Case 1	DER open-circuited
Case 2	Synchronous source as DER
Case 3	IBR as DER

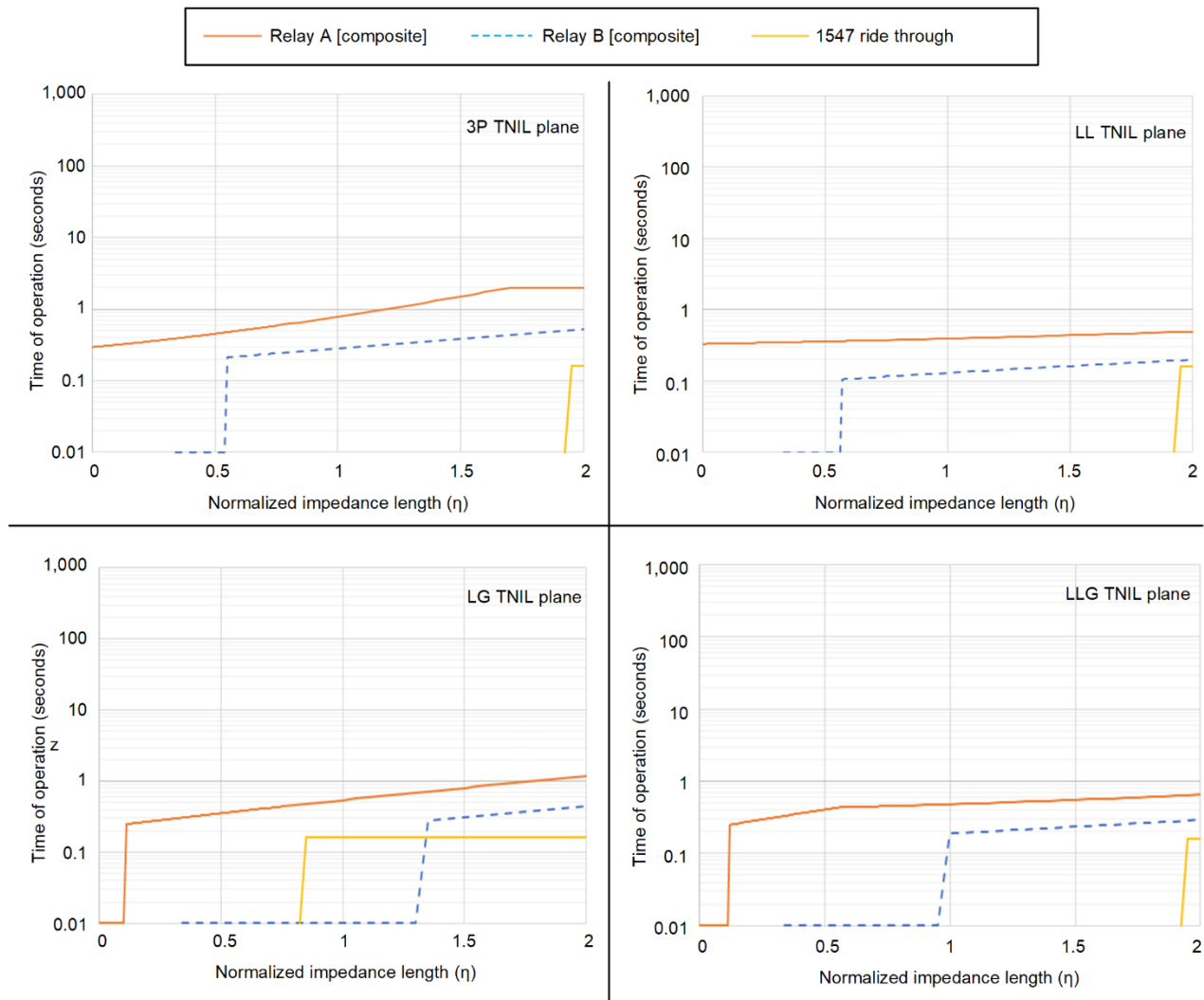


Fig. 18. Results of coordination between PCC and R4 relays.

Current-based elements on Relay B, such as 50/51P, 50/51G, and 50/51Q were modeled in MATLAB/Simulink and were loaded with the settings shown in Table IX.

In Case 1, the DER is assumed to be open-circuited, which is the assumption made in Section II to simplify the process of coordination. In Case 2, a 2 MVA synchronous generator DER source is considered to be in service at the PCC [7], which is simulated using a simplified machine model. If the DER size is comparable to the substation transformer size, the distribution system can no longer be considered radial, and the contribution of the DER source during faults must be considered. The calculation method described in the Appendix depends on the assumption that the utility (substation transformer) is much stronger than the DER source. Hence, the DER size was chosen to represent a fairly common substation transformer size to DER size ratio (12.5:2.0).

In Case 3, a 2 MW photovoltaic array with an inverter is considered to be in service at the PCC. This inverter consists of a Stage 1 maximum power point tracking-based (MPPT-based) DC-DC boost converter and a Stage 2 three-phase, three-level voltage source converter [8].

To demonstrate the dependability of the PCC relay, in all three test cases, the faults shown in Table X were simulated at the fault locations F5 and F7 (refer Fig. 3) on the interconnecting feeder. To demonstrate the selectivity of the PCC relay with area EPS relays, the same tests were repeated for the fault locations F3 and F8. As expected, the PCC relay operated for the fault locations F5 and F7, while maintaining coordination with Relays B1 and R4 for the fault locations F3 and F8, respectively.

TABLE X  
SIMULATED FAULT INFORMATION

Fault	Location	Type
F5	50% of Line B2-R2	Metallic Fault 3P, Metallic LL, and 1LG with $R_F = 5 \Omega$
F7	50% of Line R3-DER Tap	
F3	50% of Line B1-R1	
F8	50% of Line R4-R5	

In Case 2, where a synchronous generator is assumed to be in service, the time of operation of the relay changes due to the fault current contribution from the DER. Due to this contribution, the current-based elements in Relay B are faster than Case 1, while the voltage-based elements are slower than Case 1. Because Relay B is expected to be faster than Relay A, the coordination is still maintained. Therefore, for relatively smaller sizes of synchronous DER, this approach can still be used effectively. When larger (relative to utility transformer capacity) synchronous generators are used as DERs, this source can no longer be assumed to be open-circuited, and both sources have to be considered to perform the calculations necessary for coordination using directional relays.

In Case 3, the voltage source inverter is limited in its ability to provide fault current and hence does not affect the time of operation of the relays significantly. This makes an inverter-based DER an excellent application for the use of inverse-voltage-based protection at the PCC relay.

## VI. CONCLUSION

The TNIL plane offers a novel method of evaluating the speed, selectivity, and sensitivity of definite-time undervoltage protection at PCC. Inverse-time voltage relays can be combined with definite-time voltage relays at the PCC to improve speed of operation for all types of faults while maintaining coordination with area EPS relays.

Using typically available source and feeder impedances, the canonical models developed in Section III provide a means of relating voltage and current for faults at all locations along the area EPS feeder. This forms the basis of the TNIL plane. Coordination between 27/27I, 59/59I, and 50/51 elements must be established uniquely for each fault type on the TNIL plane.

When the DER includes a strong ground source, a 51G element provides better sensitivity than a 59IG element. This method of coordination can be used for inverter-based DER applications and relatively small synchronous DER applications.

## VII. APPENDIX

### A. Calculation of Operating Quantities at Relay A and Relay B for Three-Phase Faults

The objective of these calculations is to predict the operating quantities measured by Relay A and Relay B. The formulae derived in this section and in the subsequent sections can be used to perform manual or software-assisted calculations to predict the operating quantities for all types of faults that can occur at various locations ( $0 \leq \eta \leq 2$ ). Using symmetrical network analysis [6], the various operating quantities seen by Relays A and B can be calculated. In this section, a three-phase fault is considered at various locations on the protected line. Fig. 19 shows the symmetrical component network for this fault.

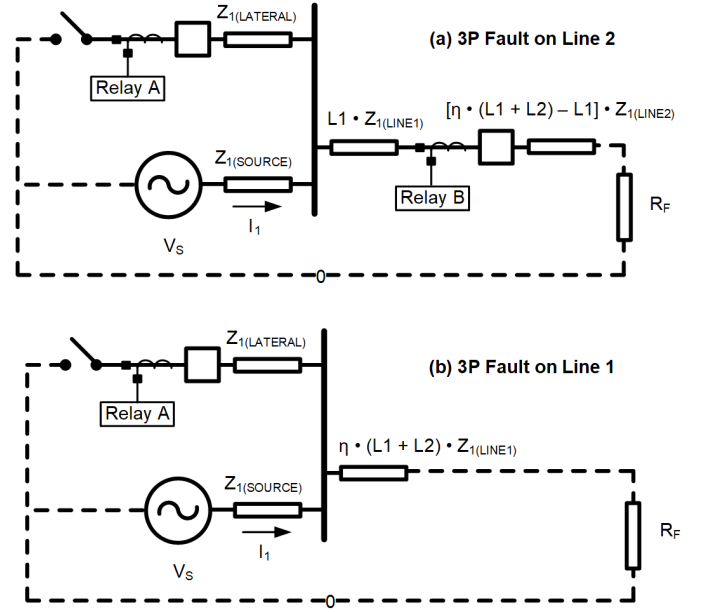


Fig. 19. Impedance networks for a 3P fault on the protected line; faults on a) Line 2 and b) Line 1 are shown.

Fig. 19a shows a 3P fault on Line 2 and the associated impedances.  $Z_{1(\text{SOURCE})}$  is the positive-sequence source impedance, based on Table VI. Similarly,  $Z_{1(\text{LINE1})}$  is the per-mile positive-sequence impedance for Line 1 and  $Z_{1(\text{LINE2})}$  is the per-mile positive-sequence impedance for Line 2. Equation (3) shows the effective positive-sequence impedance of the network in Fig. 20.  $L1$  is the length of Line 1 and  $L2$  is the length of Line 2 (in miles), given that the line impedances are in ohms/mile. Equation (4) shows the effective positive-sequence impedance of the network in Fig. 19b. For this 3P fault, Relay B measures the operating quantity as calculated in (5), while the operating quantity for Relay A is given in (6).

$$Z_1 = Z_{1(\text{SOURCE})} + L1 \cdot Z_{1(\text{LINE1})} + [\eta \cdot (L1 + L2) - L1] \cdot Z_{1(\text{LINE2})} \quad (3)$$

$$Z_2 = Z_{2(\text{SOURCE})} + L1 \cdot Z_{2(\text{LINE1})} + [\eta \cdot (L1 + L2) - L1] \cdot Z_{2(\text{LINE2})} \quad (4)$$

$$I_f = \frac{V_s}{Z_1 + R_F} \quad (5)$$

$$V_{\text{LM}(\text{MIN})} = V_s - I_f \cdot Z_{1(\text{SOURCE})} \quad (6)$$

### B. Calculation of Operating Quantities at Relay A and Relay B for LG Faults

Fig. 20a shows a LG fault on Line 2 and the associated impedances.  $Z_{1(\text{SOURCE})}$ ,  $Z_{2(\text{SOURCE})}$ , and  $Z_{0(\text{SOURCE})}$  are the positive-, negative-, and zero-sequence source impedances, respectively, based on Table V. Similarly,  $Z_{1(\text{LINE1})}$ ,  $Z_{2(\text{LINE1})}$ , and  $Z_{0(\text{LINE1})}$  are the per-mile sequence impedances for Line 1 and  $Z_{1(\text{LINE2})}$ ,  $Z_{2(\text{LINE2})}$ , and  $Z_{0(\text{LINE2})}$  are the per-mile sequence impedances for Line 2, respectively. On systems where the substation transformer creates a break in the zero-sequence impedance network (e.g., a system with a Dy1 transformer),  $Z_{0(\text{SOURCE})}$  must be chosen to disregard any impedance upstream of this transformer, because there is an open circuit.

Equations (3), (7), and (8) are used to calculate the effective sequence impedances of the network in Fig. 20a.

Equations (4), (9), and (10) are used to calculate the effective sequence impedances of the network in Fig. 20b For this LG

fault, Relay B measures the operating quantities as calculated in (11), while the operating quantities for Relay A are given in (12), (13), and (14).

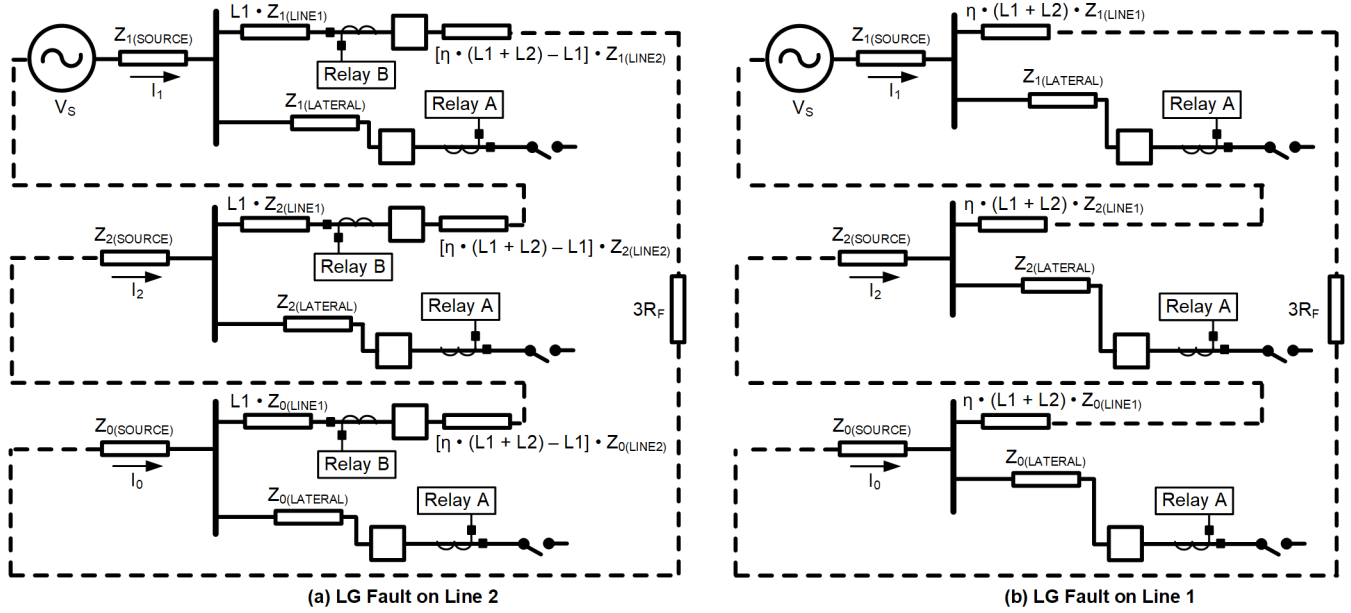


Fig. 20. Impedance networks for an LG fault on the protected line; faults on a) Line 2 and b) Line 1 are shown.

$$Z_2 = Z_{2(\text{SOURCE})} + L1 \cdot Z_{2(\text{LINE}1)} + [\eta \cdot (L1 + L2) - L1] \cdot Z_{2(\text{LINE}2)} \quad (7)$$

$$Z_0 = Z_{0(\text{SOURCE})} + L1 \cdot Z_{0(\text{LINE}1)} + [\eta \cdot (L1 + L2) - L1] \cdot Z_{0(\text{LINE}2)} \quad (8)$$

$$Z_2 = Z_{2(\text{SOURCE})} + \eta \cdot (L1 + L2) \cdot Z_{2(\text{LINE}1)} \quad (9)$$

$$Z_0 = Z_{0(\text{SOURCE})} + \eta \cdot (L1 + L2) \cdot Z_{0(\text{LINE}1)} \quad (10)$$

$$I_f = 3I_0 = 3I_2 = 3I_1 = \frac{3 \cdot V_S}{Z_1 + Z_2 + Z_0 + 3 \cdot R_F} \quad (11)$$

$$3V_2 = -Z_{2(\text{SOURCE})} \cdot 3I_2 \quad (12)$$

$$3V_0 = -Z_{0(\text{SOURCE})} \cdot 3I_0 \quad (13)$$

$$V_{\text{LN(MIN)}} = V_0 + V_S - I_1 \cdot Z_{1(\text{SOURCE})} + V_2 \quad (14)$$

### C. Calculation of Operating Quantities at Relay A and Relay B for LL Faults

Fig. 21 shows the symmetrical component network for a LL fault at various locations on the protected line.

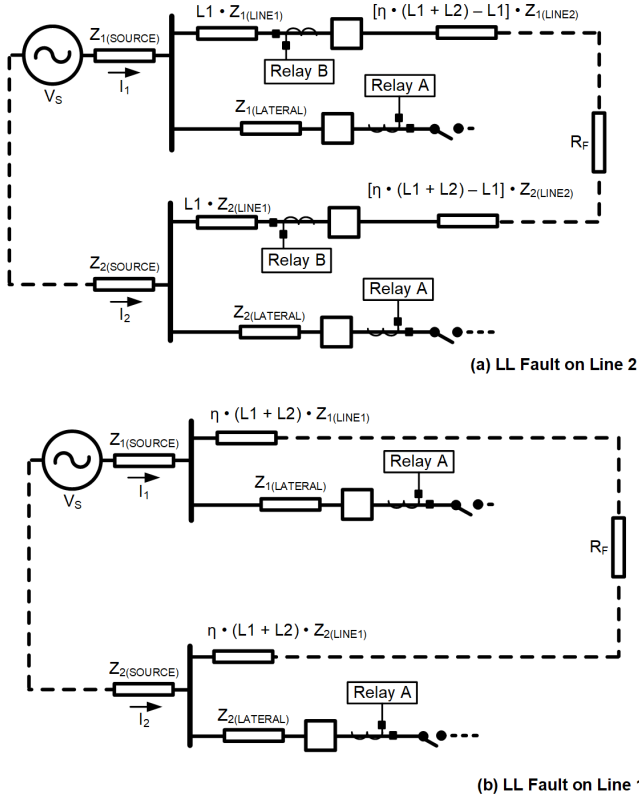


Fig. 21. Impedance network for an LL fault on Topology B coordination pairs.

Equations (3) and (7) are used to calculate the effective sequence impedances of the network in Fig. 21a. Equations (4) and (9) are used to calculate the effective sequence impedances of the network in Fig. 21b. For this LL fault, Relay B measures the operating quantities as calculated in (15) and (16), while the operating quantities for Relay A are given in (12) and (17). In the following equations, “a” refers to a unit phasor with an angle of  $120^\circ$  ( $1\angle 120$ ). Equation (18) calculates the minimum line-to-line voltage during line-to-line faults, which is used to determine the minimum ride-through requirement.

$$3I_2 = -3I_1 = \frac{-3 \cdot V_S}{Z_1 + Z_2 + R_F} \quad (15)$$

$$I_F = I_2 \sqrt{3j} \quad (16)$$

$$V_{LN(\text{MIN})} = a^2(V_S - I_1 \cdot Z_{I(\text{SOURCE})}) + a \cdot V_2 \quad (17)$$

$$V_{LL(\text{MIN})} = (a^2 - a)(V_S - I_1 \cdot Z_{I(\text{SOURCE})} - V_2) \quad (18)$$

### D. Calculation of Operating Quantities at Relay A and B for LLG faults

Fig. 22 shows the symmetrical component network for a LLG fault at various locations on the protected line. Equations (3), (7), and (8) are used to calculate the effective sequence impedances of the network in Fig. 21a. Equations (4), (9), and (10) are used to calculate the effective sequence impedances of the network in Fig. 21b.  $Z_{\text{EFF}}$  is defined as the combined impedance of the parallel-connected negative- and zero-sequence impedance networks and the series-connected positive-sequence impedance and is derived in (19).

Equation (20) calculates the positive-sequence current. For this LLG fault, Relay B measures operating quantities as calculated in (21), (22), and (23). Equations (12), (13), and (24) are used to calculate the operating quantities for Relay A. Equation (18) can be used to calculate the minimum line-to-line voltage, which is used to determine the minimum ride-through requirement.

$$Z_{\text{EFF}} = Z_1 + \frac{Z_2 \cdot (Z_0 + 3R_F)}{Z_2 + Z_0 + 3R_F} \quad (19)$$

$$I_1 = \frac{V_S}{Z_{\text{EFF}}} \quad (20)$$

$$3I_2 = -3I_1 \cdot \left( \frac{Z_0 + 3R_F}{Z_2 + Z_0 + 3R_F} \right) \quad (21)$$

$$3I_0 = -3I_1 \cdot \left( \frac{Z_2}{Z_2 + Z_0 + 3R_F} \right) \quad (22)$$

$$I_f = I_0 + a^2 I_1 + a I_2 \quad (23)$$

$$V_{LN(\text{MIN})} = a^2(V_S - I_1 \cdot Z_{I(\text{SOURCE})}) + a V_2 + V_0 \quad (24)$$

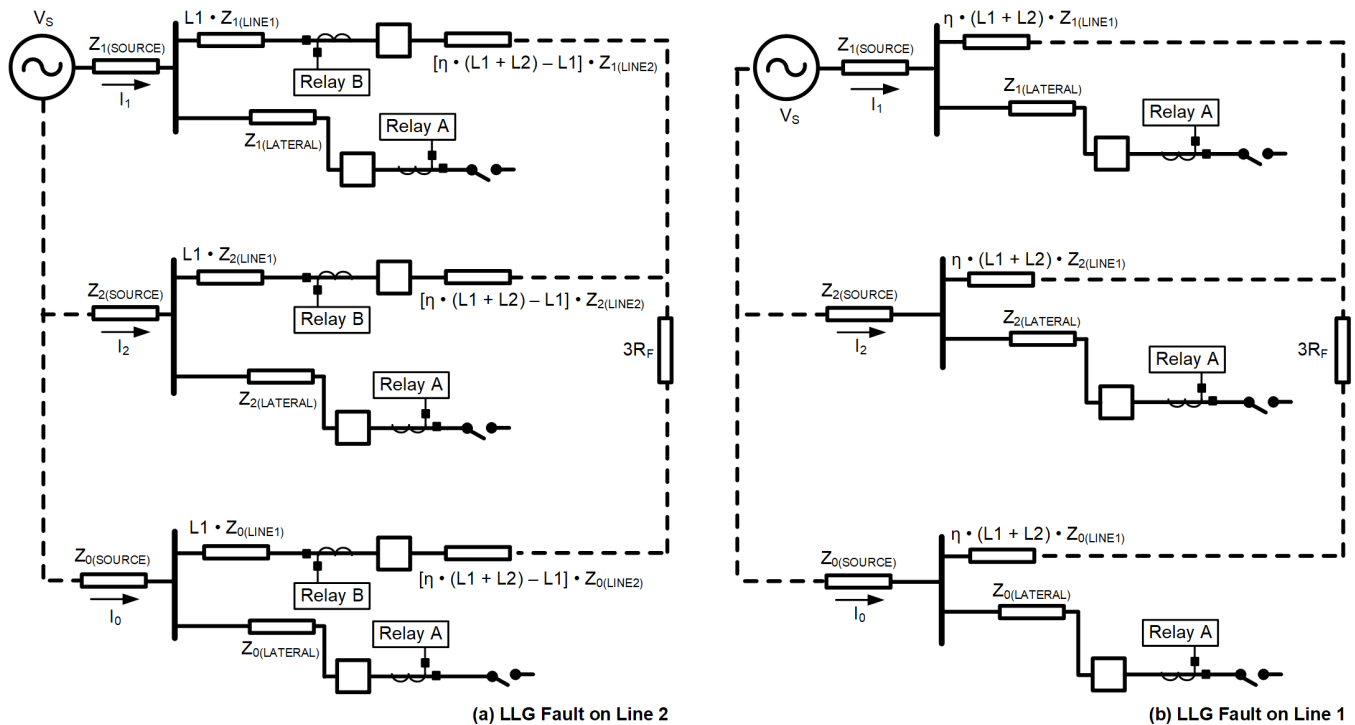


Fig. 22. Impedance networks for an LLG fault on the protected line. Faults on a) Line 2 and b) Line 1 are shown.

#### E. Calculation of Operating Quantities for Relay A and B for LLG faults with a Zero-Sequence Source at the PCC

Fig. 23 shows the fault impedance network for an LLG fault on the protected line. In this model, the zero-sequence impedance of the delta-wye-grounded transformer (or zigzag transformer) at the PCC is included in the fault impedance network. Subsequently, the zero-sequence impedance of the lateral line now plays an active in the calculations. The DER is still assumed to be open-circuited and the effect of load is still ignored, so the positive- and negative-sequence impedances of

the lateral feeder are open-circuited, and hence, have no influence in the fault impedance network.

$Z_{0(LATERAL)}$  is the zero-sequence impedance of the lateral line, while  $Z_{0(XFMR)}$  is the zero-sequence impedance of the interconnecting grounding transformer for this distribution system example, as illustrated in the canonical model shown in Fig. 14. Equations (3), (7), and (24) are used to calculate the effective sequence impedances of the network in Fig. 23a.

Equations (4), (9), and (25) are used to calculate the effective sequence impedances of the network in Fig. 23b. Equation (18) is used to derive  $Z_{EFF}$ .

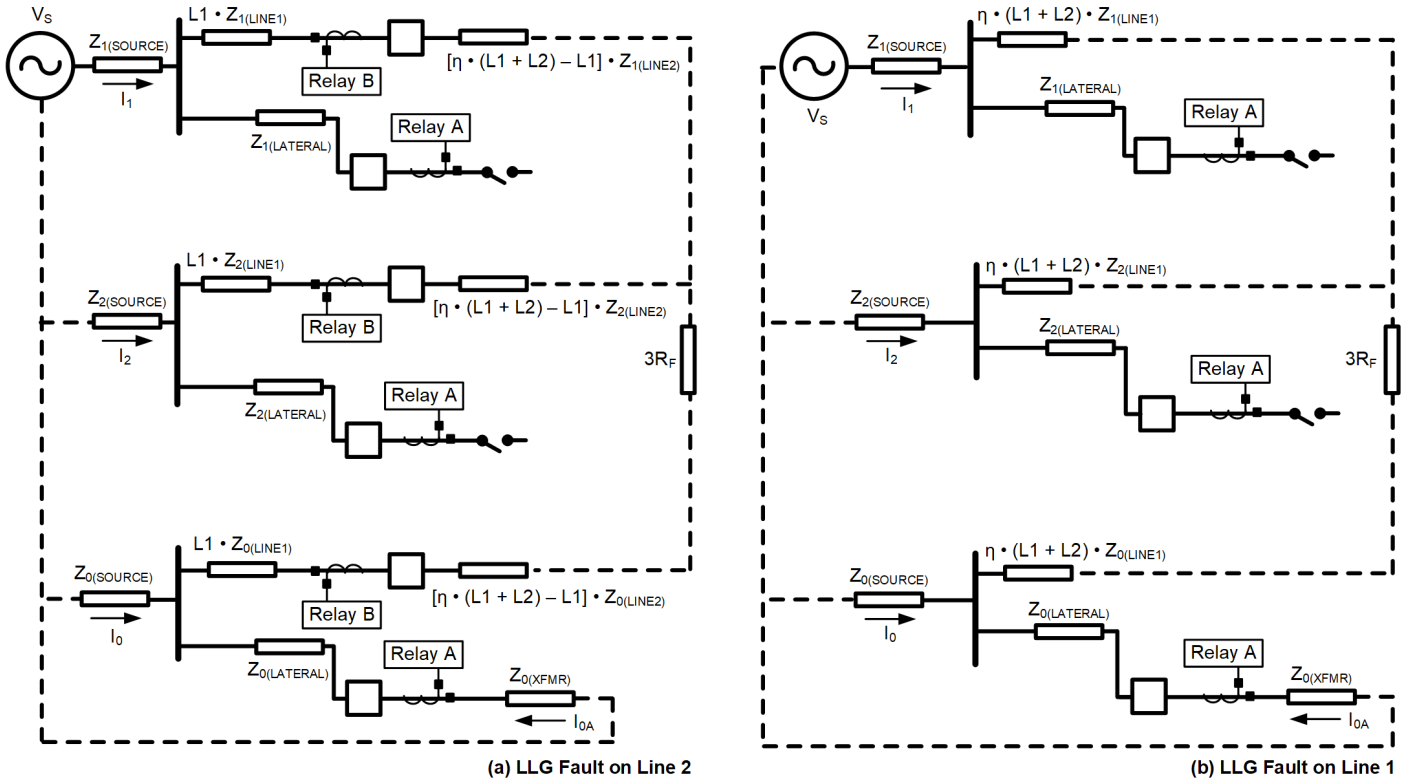


Fig. 23. Impedance networks for an LLG fault on the protected line with a zero-sequence source at the PCC; faults on a) Line 2 and b) Line 1 are shown.

$$Z_0 = \frac{Z_{0(\text{SOURCE})} \cdot (Z_{0(\text{LATERAL})} + Z_{0(\text{XFMR})})}{Z_{0(\text{SOURCE})} + Z_{0(\text{LATERAL})} + Z_{0(\text{XFMR})}} + L1 \cdot Z_{0(\text{LINE1})} + [\eta \cdot (L1 + L2) - L1] \cdot Z_{0(\text{LINE2})} \quad (25)$$

$$Z_0 = \frac{Z_{0(\text{SOURCE})} \cdot (Z_{0(\text{LATERAL})} + Z_{0(\text{XFMR})})}{Z_{0(\text{SOURCE})} + Z_{0(\text{LATERAL})} + Z_{0(\text{XFMR})}} + \eta \cdot (L1 + L2) \cdot Z_{0(\text{LINE1})} \quad (26)$$

$$3V_0 = -Z_{0(\text{XFMR})} \cdot 3I_0 \cdot \left( \frac{Z_{0(\text{SOURCE})}}{Z_{0(\text{SOURCE})} + Z_{0(\text{LATERAL})} + Z_{0(\text{XFMR})}} \right) \quad (27)$$

$$3I_{0A} = 3I_0 \cdot \left( \frac{Z_{0(\text{SOURCE})}}{Z_{0(\text{SOURCE})} + Z_{0(\text{LATERAL})} + Z_{0(\text{XFMR})}} \right) \quad (28)$$

Equation (20) calculates the positive-sequence current. For this LLG fault, Relay B measures operating quantities as calculated in (21), (22), and (23). Equations (12), (24), (27), and (28) are used to calculate the operating quantities for Relay A. Equation (18) can be used to calculate the minimum line-to-line voltage, which is used to determine the minimum ride-through requirement.

#### F. Calculation of Operating Quantities for Relay A and B for LG faults with a Zero-Sequence Source at the PCC

Fig. 24 shows the fault impedance network for an LG fault on the protected line with a delta-wye-grounded transformer (or zigzag transformer) at the PCC. Similar to the calculations in

Appendix E, the zero-sequence impedance of the lateral line is now included in the calculations as the lateral line can no longer be assumed to be open-circuited.

Equations (3), (7), and (25) are used to calculate the effective sequence impedances of the network in Fig. 24a.

Equations (4), (9), and (26) show the effective sequence impedances of the network in Fig. 24b. For this LG fault, Relay B measures the operating quantities as calculated in (11), while the operating quantities for Relay A are given in (12), (14), (27), and (28).

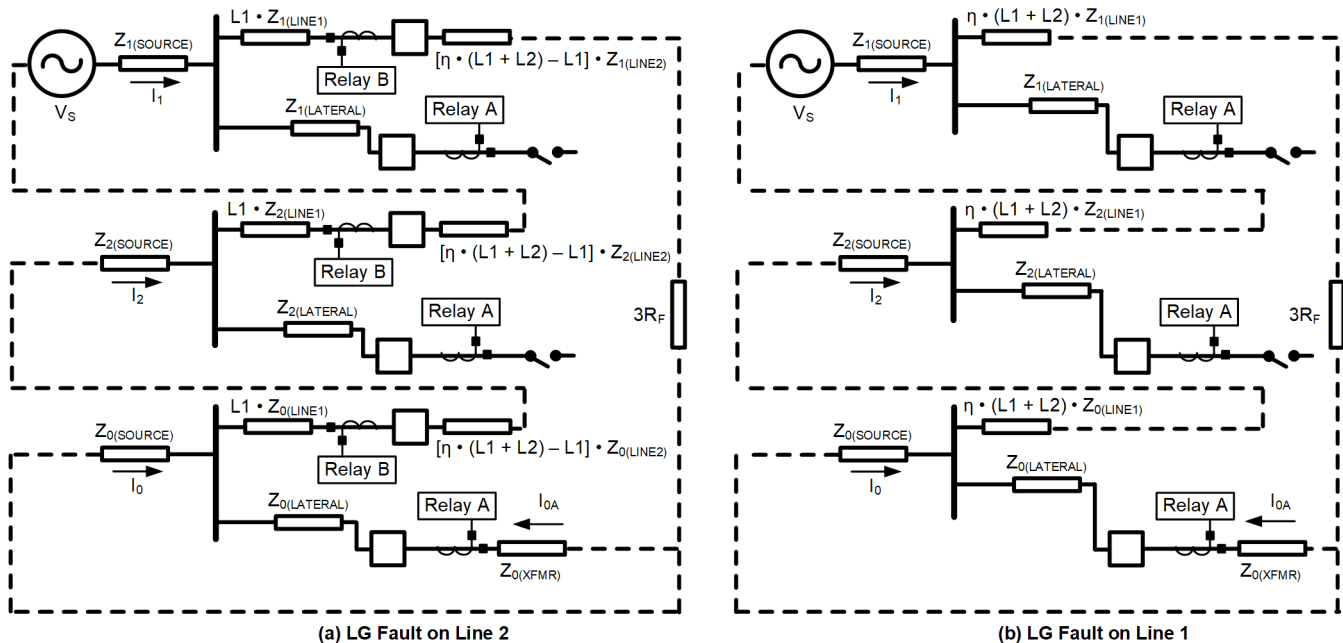


Fig. 24. Impedance networks for an LG fault on the protected line; faults on a) Line 2 and b) Line 1 are shown.

## VIII. REFERENCES

- [1] R. Chowdhury and N. Fischer, "Transmission Line Protection for Systems With Inverter-Based Resources – Part I: Problems," *IEEE Transactions on Power Delivery*, Vol. 36, Issue 4, August 2021, pp. 2416-2425.
- [2] IEEE Std. C37.102, *IEEE Guide for AC Generator Protection*, 2006.
- [3] IEEE Std 1547, *IEEE Standard for Interconnection and Interoperability of Distributed Energy Resources with Associated Electric Power Systems Interfaces*, 2018.
- [4] G. Benmouyal, A. Guzmán, and R. Jain, "Tutorial on the Impact of Network Parameters on Distance Element Resistance Coverage," proceedings of the 40th Annual Western Protective Relay Conference, Spokane, WA, October 2013.
- [5] SEL-751 *Feeder Protection Relay Instruction Manual*.
- [6] J. L. Blackburn and T. J. Domin, *Protective Relaying: Principles and Applications*, 4th edition, CRC Press, Boca Raton, FL, 2014.
- [7] G. Sybille, "Simplified Synchronous Machine – Speed Regulation," MathWorks, 2022. Available: [mathworks.com/help/physmod/sps/ug/simplified-synchronous-machine-speed-regulation.html;jsessionid=3625db551c3b2eac869e1828d3e1](https://mathworks.com/help/physmod/sps/ug/simplified-synchronous-machine-speed-regulation.html;jsessionid=3625db551c3b2eac869e1828d3e1).
- [8] P. Giroux, G. Sybille, C. Osorio, and S. Chandrchood, "Average Model of a 100-kW Grid-Connected PV Array," MathWorks. Available: [mathworks.com/help/physmod/sps/ug/average-model-of-a-100-kw-grid-connected-pv-array.html](https://mathworks.com/help/physmod/sps/ug/average-model-of-a-100-kw-grid-connected-pv-array.html).

## IX. BIOGRAPHIES

**Jai Subbarayan** graduated from the National Institute of Technology, Tiruchirappalli, India, in 2016 with a Bachelor of Technology in electrical and electronics engineering with honors, following which he worked for the Dow Chemical Company as an electrical engineer. Jai graduated from North Carolina State University with an MSc in electric power systems engineering in 2019 and joined Schweitzer Engineering Laboratories, Inc. (SEL) as a protection application engineer.

**Brett Cockerham** earned his BSc in electrical engineering technology, summa cum laude, in 2014 and his MSc in applied energy and electromechanical systems in 2016. Both degrees were awarded by the University of North Carolina at Charlotte. In 2014, Brett joined Schweitzer Engineering Laboratories, Inc. (SEL) as an application engineer focusing on power system protection and control.

**Jeremy Blair**, PE, joined Schweitzer Engineering Laboratories, Inc. (SEL) as an application engineer in 2013, authoring conference papers and application guides and assisting customers with relay and distribution automation solutions. Previously, he worked for Entergy Corporation as a distribution planning engineer with responsibilities in distribution system planning, protection, power quality, and automation in Baton Rouge, Louisiana. He also managed Entergy's automatic load transfer and sectionalization program over its four-state territory. Jeremy earned his BSEE from Louisiana Tech University and his MSECE from Georgia Institute of Technology. He is a licensed professional engineer in the state of Louisiana.